UNIVERSITI PUTRA MALAYSIA

STRUCTURAL AND OPTICAL PROPERTIES OF PbS AND PbS/MnTe CORE/SHELL QUANTUM DOTS

NUR DIYANA BINTI HALIM

FS 2022 13

STRUCTURAL AND OPTICAL PROPERTIES OF PbS AND PbS/MnTe CORE/SHELL QUANTUM DOTS

By

NUR DIYANA BINTI HALIM

Thesis is submitted to the School of Graduate Studies, Universiti Putra Malaysia, in Fulfilment of the Requirements for the Degree of Master of Science

November 2021

Abstract of thesis presented to the Senate of Universiti Putra Malaysia in fulfilment of the requirement for the degree of Master of Science

STRUCTURAL AND OPTICAL PROPERTIES OF PbS AND PbS/MnTe CORE/SHELL QUANTUM DOTS

By

NUR DIYANA BINTI HALIM

November 2021

Chairman : Mazliana Binti Ahmad Kamarudin, PhD
Faculty : Science

The optical properties of colloidal quantum dots (QDs) are affected by the size of QDs, material used and the capping agents. This thesis explores on the study of PbS/MnTe core/shell QDs where PbS acts as the core and MnTe is the shell. The QDs had been synthesized at ambient temperature by using aqueous synthesis approach. The PbS/MnTe core/shell QDs with different shell thickness (0.3, 0.6 and 0.9 monolayer (ML)) were effectively fabricated in this study.

The structural and optical characteristics of PbS QDs and PbS/MnTe core/shell QDs are also studied in this study. High-Resolution Transmission Electron Microscopy (HRTEM) and Energy Dispersive X-ray Microscopy (EDX) have been used to investigate the structural characteristics of QDs sample. According to HRTEM analysis, the average size of the PbS QDs was 4.46 ± 0.82 nm, with a spherical form. The average size of PbS/MnTe core shell QDs was increased to 4.80 ± 0.73 nm for PbS/MnTe 0.3 ML, 5.16 ± 0.80 nm for PbS/MnTe 0.6 ML and 5.53 ± 0.84 nm for PbS/MnTe 0.9 ML, respectively. The size core/shell QDs was enhanced because of the growth of MnTe shell on PbS core. Aside from that, the analysis of EDX has been performed on the samples of PbS and PbS/MnTe core/shell QDs to prove the existence of MnTe elements. The peak in EDX spectrum related with Mn and Te was identified at 5.9 keV and 3.7 keV.

Photoluminescence (PL) spectroscopy was used to explore the optical characteristics and behaviour of charge carriers within PbS and PbS/MnTe QDs at various temperatures (10-300 K). The PL peak energies of PbS/MnTe core shell QDs at room temperature were blue-shifted as the shell thickness increased due to the strong confinement effect caused by presence of MnTe shell. The effect of temperature on the PL peak energy, full width half maximum (FWHM), and PL intensity can be observed in the temperature dependent PL. In general, the PL peak energy and FWHM increase monotonically as temperature

increased, owing to the interaction of charge carriers with phonons. In contrast, as the temperature increased, the PL peak intensities decreased, which was related with the excitation of carriers out of the QDs into non-radiative recombination centres. The research and production PbS/MnTe core/shell QDs would be valuable in the coming decades particularly in the application of photovoltaic devices.

Abstrak tesis yang dikemukakan kepada Senat Universiti Putra Malaysia sebagai memenuhi keperluan untuk ijazah Master Sains

SIFAT STRUKTUR DAN OPTIK TERAS DALAMAN KUANTUM DOTS PbS DAN PbS/MnTe

By

NUR DIYANA BINTI HALIM

November 2021

Pengerusi : Mazliana Binti Ahmad Kamarudin, PhD
Fakulti : Sains

Sifat optik titik kuantum koloid dipengaruhi oleh ukuran saiz titik, bahan yang digunakan dan molekul penutup. Tesis ini meneroka kajian mengenai teras dalaman-luaran titik kuantum PbS/MnTe di mana PbS bertindak sebagai teras dan MnTe adalah lapisan luaran. Titik kuantum koloid telah disintesis pada suhu persekitaran bilik dengan menggunakan pendekatan sintesis akua. Teras dalaman-luaran titik kuantum PbS/MnTe dengan ketebalan lapisan MnTe yang berbeza (0.3, 0.6 dan 0.9 lapisan mono (ML)) telah dihasilkan secara berkesan dalam kajian ini.

Ciri struktur dan pencirian optik titik kuantum koloid PbS dan PbS/MnTe juga dikaji dalam penyelidikan ini. Mikroskopi elektron transmisi resolusi tinggi (HRTEM) dan mikroskopi penyebaran tenaga X-ray (EDX) telah digunakan untuk menyiasat ciri struktur semua sampel titik kuantum. Berdasarkan analisis HRTEM, ukuran purata saiz titik kuantum koloid PbS adalah 4.46 ± 0.82 nm, serta berbentuk sfera. Saiz purata teras dalaman-luaran titik kuantum PbS/MnTe bertambah kenaikannya menjadi 4.80 ± 0.73 nm untuk PbS/MnTe 0.3 ML, 5.16 ± 0.80 nm untuk PbS / MnTe 0.6 ML dan 5.53 ± 0.84 nm untuk PbS / MnTe 0.9 ML masing-masing. Purata saiz teras dalaman-luaran titik kuantum meningkat kerana pertumbuhan lapisan MnTe pada teras PbS. Selain itu, analisis EDX telah dilakukan pada sampel PbS dan PbS/MnTe untuk membuktikan kewujudan komposisi MnTe. Puncak dalam spektrum EDX yang berkaitan dengan komposisi Mn dan Te dikenal pasti pada 5.9 keV dan 3.7 keV.

Spektroskopi fotoluminesens (PL) digunakan untuk meneroka ciri optik dan tingkah laku pembawa cas dalam PbS dan PbS/MnTe pada pelbagai suhu (10-300 K). Tenaga puncak PL titik kuantum teras-dalaman PbS/MnTe pada suhu bilik bertukar biru kerana ketebalan lapisan meningkat disebabkan oleh kesan pengurungan yang kuat disebabkan oleh kehadiran lapisan MnTe. Kesan suhu

pada tenaga puncak PL, lebar penuh ketinggian maksimum (FWHM), dan keamatan PL dapat diperhatikan pada PL yang bergantung pada suhu. Secara umum, tenaga puncak PL dan FWHM meningkat secara berkala ketika suhu meningkat, disebabkan oleh interaksi pembawa cas dengan fonon. Sebaliknya, ketika suhu meningkat, keamatan puncak PL menurun, yang terkait dengan pengujaan pembawa yang keluar dari titik kuantum kepada pusat penggabungan bukan radiasi. Penyelidikan dan pengeluaran titik kuantum teras-dalaman PbS/MnTe akan sangat berharga dalam beberapa dekad yang akan datang terutamanya dalam penggunaan peranti fotovoltaik.

ACKNOWLEDGEMENT

In awareness that this work could not be finished without the God willing, hereby "Praise to be God, the Lord of the World". It is a pleasure to give my deepest gratitude to my research supervisor, Dr Mazliana Ahmad Kamarudin for all her assistance, ideas, supervision and encouragement throughout my master research. Furthermore, I want to thank my co supervisors, Dr Josephine Liew Ying for her support and assistance to finish my research this year. Special thanks to my great friends, my lab mates, Safwan Zaini and Hani Syazlin whose gave me their hand and encouragement during accomplished this project. I wish all of you all the best in your life. Last but not least, I want to express my gratitude to my family especially my parents for their love, immense patience and diligence to support me. Words cannot explain my love and thanks to them.

I certify that a Thesis Examination Committee has met on 29 November 2021 to conduct the final examination of Nur Diyana binti Halim on her thesis entitled Structural and Optical Properties of PbS And PbS/MnTe Core/Shell Quantum Dots in accordance with the Universities and University Colleges Act 1971 and the Constitution of the Universiti Putra Malaysia [P.U.(A) 106] 15 March 1998. The Committee recommends that the student be awarded the Master of Science.

Members of the Thesis Examination Committee were as follows:

Mohd Mustafa Awang Kechik, PhD
Associate Professor
Faculty of Science
Universiti Putra Malaysia
(Chairman)

Chen Soo Kien, PhD
Associate Professor
Faculty of Science
Universiti Putra Malaysia
(Internal Examiner)

Dee Chang Fu, PhD
Associate Professor
Institute of Microengineering and Nanoelectronics (IMEN)
Universiti Kebangsaan Malaysia
Malaysia
(External Examiner)

ZANARIAH ABDUL MAJID, PhD
Professor and Deputy Dean
School of Graduate Studies
Universiti Putra Malaysia

Date: 31 March 2022

This thesis was submitted to the Senate of Universiti Putra Malaysia and has been accepted as fulfilment of the requirement for the degree of Master of Science The members of the Supervisory Committee were as follows:

Mazliana binti Ahmad Kamarudin, PhD
Senior Lecturer
Faculty of Science
Universiti Putra Malaysia
(Chairman)

Josephine Liew Ying Chyi, PhD
Senior Lecturer
Faculty of Science
Universiti Putra Malaysia
(Member)

____
ZALILAH MOHD SHARIFF, PhD

Professor and Dean
School of Graduate Studies
Universiti Putra Malaysia

Date: 14 April 2022

Declaration by Members of Supervisory Committee

This is to confirm that:

- the research and the writing of this thesis were done under our supervision;
- supervisory responsibilities as stated in the Universiti Putra Malaysia (Graduate Studies) Rules 2003 (Revision 2015-2016) are adhered to.

Signature:
Name of Chairman of Supervisory Committee: Mazliana Ahmad Kamarudin

Signature:
Name of Member of Supervisory Committee: Josephine Liew Ying Chyi

TABLE OF CONTENTS

	Page
ABSTRACT	i
ABSTRAK	iii
ACKNOWLEDGEMENT	v
APPROVAL	viii
DECLARATION	xi
LIST OF TABLES	xii
LIST OF FIGURES	xiii
LIST OF ABBREVIATIONS	xv

CHAPTER

1	**INTRODUCTION**	1
	1.1 Background of Study	1
	1.2 Importance of Problem Statement	6
	1.3 Research Objectives	8
2	**LITERATURE REVIEW**	9
	2.1 Quantum Dots	9
	2.2 Quantum Confinement Effect	10
	2.3 Quantum Dots Material	12
	2.4 Methods of Synthesis Quantum Dots	14
	2.5 Core/shell QDs	16
3	**METHODOLOGY**	20
	3.1 Sample Preparation	20
	3.1.1 PbS quantum dots	20
	3.1.2 PbS/MnS quantum dots	21
	3.2 Characterisation	26
	3.2.1 Transmission Electron Microscopy	26
	3.2.2 Energy Dispersive X-ray	27
	3.2.3 Photoluminescence spectroscopy	28
	3.3 Error Analysis	30
4	**RESULT AND DISCUSSION**	31
	4.1 Structural Characterisation	31
	4.1.1 High Resolution Transmission Electron Microscopy Analysis	31
	4.1.2 Energy Dispersive X-ray Analysis	35
	4.2 Optical Characterisation	38
	4.2.1 Photoluminescence at room temperature	38
	4.2.2 Temperature dependent photoluminescence of PbS	41
	4.2.3 Temperature dependent photoluminescence of PbS/MnTe	46

5	**CONCLUSION**	53
	5.1 Conclusion	53
	5.2 Future Works	54
	REFERENCES	56
	BIODATA OF STUDENT	67
	LIST OF PUBLICATION	68

LIST OF TABLES

Table		Page
1.1	Nanomaterials are classified as 3D, 2D, 1D and 0D which according to their density of state and quantum confinement.	4
2.1	Type of QDs.	12
3.1	Materials used to prepare PbS QDs.	21
3.2	Materials used to prepare MnTe shell layer.	22
3.3	The amount of MnTe had been injected into PbS.	23
4.1	Size of QDs measured by HRTEM.	34
4.2	EDX data for sample PbS and PbS/MnTe QDs indicating atomic %.	36
4.3	The value parameters of equation (4.2) for PbS QDs.	43
4.4	The value parameters of equation (4.3) for PbS QDs.	44
4.5	The value parameters of equation (4.3) for PbS/MnTe 0.3ML QDs.	47
4.6	The value of temperature coefficeint for PbS QDs and PbS/MnTe core/shell QDs with different shell thickness.	49
4.7	The value of parameters based on equation (4.2) for PbS QDs and PbS/MnTe core/shell QDs with different shell thickness (0.3 – 0.9 ML).	50
4.8	The value of parameters based on equation (4.3) for PbS QDs and PbS/MnTe core/shell QDs with different shell thickness (0.3 – 0.9 ML)	52

LIST OF FIGURES

Figure		Page
1.1	QDs emit at colour in the region of visible wavelength (Han *et al*., 2014).	5
1.2	The figure shows the cross-sectional image of core/shell QDs.	6
2.1	The mechanism of exciton formation in bulk material.	10
2.2	High-resolution TEM image of CdSe QDs dispersed uniformly in the chloroform solution.	15
2.3	The figure shows the cross-sectional image of core/shell QDs	16
2.4	Structure of the energy level arrangement in (a) type-I, (b) inverse type-I, (c) type-II and (d) quasi type-II core/shell QDs.	17
2.5	Absorption spectra of the CdSe, CdS and CdSe/CdS QDs.	18
2.6	The fluorescence spectra CdTe QDs and CdTe/CdSe core/shell QDs with different thickness of shell (Yang *et al*., 2011).	19
3.1	The schematic procedure of synthesis PbS QDs.	24
3.2	The schematic procedure of synthesis PbS/MnTe core/shell QDs.	25
3.3	The illustration of how TEM operated.	26
3.4	Schematic figure of experimental setup used in PL studies.	29
4.1	HRTEM images of PbS QDs at different magnifications.	31
4.2	HRTEM images of PbS/MnTe 0.3 ML at various magnifications (a) 100 nm (b) 10 nm.	32
4.3	HRTEM image of PbS/MnTe samples with (a) 0.6 ML and (b) 0.9 ML shell thickness.	33
4.4	EDX spectrum of PbS QDs, showing the peak of each elements composed in the sample.	35

4.5 EDX spectrum of PbS/MnTe core/shell QDs with different monolayer (a) PbS/MnTe 0.3 ML, (b) PbS/MnTe 0.6 ML and (c) PbS/MnTe 0.9 ML. 37

4.6 PL peak energy spectrum of PbS QDs was observed at E_{gap} = 1.06 eV as compared with bulk PbS. 39

4.7 Room temperature of PL properties of PbS and PbS/MnTe core/shell QDs (a) PL spectra, (b) PL peak energy (c) FWHM and (d) PL intensity. 40

4.8 Temperature dependence of PL properties of PbS QDs. a) Full PL spectra b) PL peak energy, c) FWHM and d) integrated PL intensity. 41

4.9 PL temperature dependence of PbS/MnTe 0.3 ML QDs. a) PL spectra b) PL peak energy, c) FWHM and d) integrated PL intensity. 46

4.10 Temperature dependence of PL peak position of PbS QDs and PbS/MnTe core/shell QDs with different shell thickness (0.3 ML – 0.9 ML). 48

4.11 Temperature dependence of FWHM of PbS QDs and PbS/MnTe core/shell QDs with different shell thickness (0.3 ML – 0.9 ML). 49

4.12 Temperature dependence of integrated PL intensity of PbS QDs and PbS/MnTe core/shell QDs with different shell thickness (0.3 ML – 0.9 ML). 51

LIST OF ABBREVIATIONS

QDs	Quantum Dots
PbS	Lead sulphide
MnTe	Manganese telluride
ML	Monolayer
eV	Electron volt
HRTEM	High-Resolution Transmission Electron Microscopy
EDX	Energy Dispersive X-ray Microscopy
PL	Photoluminescence
FWHM	Full width half maximum
ZnS	Zinc sulphide
GaAs	Gallium arsenide
QLED	Quantum light emitting diodes
DOS	Density of states
3D	Three-dimensional
2D	Two-dimensional
1D	One-dimensional
0D	Zero-dimensional
ZnTe	Zinc telluride
CdSe	Cadmium selenide
InAs	Indium arsenide
NIR	Near-infrared
CdS	Cadmium sulphide
CdTe	Cadmium tellurite
CuCl	Copper chloride

MnS	Manganese sulphide
$MnSO_4$	Manganese (II) sulphate
$MnCl_2$	Manganese chloride
ODE	Octadene
OA	Oleic Acid
QY	Quantum Yield
PbSe	Lead selenide
PbTe	Lead telluride
MPA	Mercaptopropionic acid
TGL	Thiolglycerol
DTG	Dithiolglycerol
VB	Valence Band
CB	Conduction Band

CHAPTER 1

INTRODUCTION

1.1 Background of study

Nanomaterials are substances of a small size, ranging from 1 to 1000 nanometres. Nanomaterials have a major impact on the world because their size at the nanoscale can modify the optical, electrical and mechanical properties (Zhang *et al*.,2016; Ogaili *et al*., 2020). The size and structure of nanomaterials have a significant impact on their physical and chemical characteristics. Nanomaterials contain a higher fraction of surface atoms than bulk materials, which affects their characteristics. Shape-dependent features of nanomaterials are beneficial in applications such as catalysis, data storage, and optics. Shape-dependent characteristics are a difficult subject to research. The conductivity, melting point, optical, electrical, and mechanical properties are all affected when the size of substances is reduced.

For example, the spatial quantum confinement effect affects the optical characteristics of semiconductor nanoparticles significantly (Chen *et al*., 2013). Similarly, the high surface-to-volume ratio has a significant impact on their optical and surface characteristics. As a result, semiconductor nanomaterials have gotten a lot of interest in terms of research and applications in fields including energy conversion, sensing, electronics, photonics, and biomedicine. Sarojini *et al*. (Sarojini *et al*., 2013) conducted a major study on the electrical conductivity of nanofluids comprising metallic or oxide nanoparticles (Cu, Al2O3, and CuO) of various low-volume fractions and particle sizes. The electrical conductivity improves with increasing particle concentration and decreases with decreasing particle size, according to the authors.

Many researchers have created a large number of nanomaterials such as zinc sulphide (ZnS) nanowires (Hu *et al*., 2015), gallium arsenide (GaAs) quantum wells (Haldar *et al*., 2017) and lead sulphide (PbS) quantum dots (Su *et al*., 2017) in order to address a wide range of nanotechnology applications in recent decades. Quantum light emitting diodes (QLED) smart televisions, which have become commercially available, are an example of display technology that employs quantum dots as a nanomaterial.

Nanomaterials are classified as two-dimensional (2D), one-dimensional (1D) or zero-dimensional (0D) systems. It was classified based on free carrier motion which is limited to one, two and zero spatial dimension. Understanding the density of states (DOS) idea might help to identify how nanostructures form (Knott, 2013). DOS is referred to the number of electronic states allowed to be occupied per duration of energy (Imai *et al*., 2001).

In the last decades, the fabrication of low-dimensional semiconductor structures has made progress to reduce the effective dimension from 3D to 2D, 1D, and 0D. The progress can be observed from the derivation of density of state (DOS) and quantum confinement effect of the quantum dimensions (3D, 2D, 1D and 0D).

Bulk materials are used to classify as 3D systems. The parabolic energy dispersion for the DOS per unit volume in 3D is given by equation (1.1):

$$D(E) = \frac{1}{2\pi^2}\left(\frac{2m^*}{\hbar^2}\right)^{\frac{3}{2}}\sqrt{E_g - E} \qquad (1.1)$$

where m^* is the electron mass, E is the energy and $\hbar$ is the Planck's constant. Because DOS is proportional to $E^{1/2}$, the electron can be occupied at the continuous energy level, as shown in Table 1.1.

In the 2D system, the electron can move freely in two directions but is only confined in one. The DOS of this system can be shown by equation (1.2):

$$D(E) = \frac{m_e^*}{\pi\hbar^2}\sigma\left(E_g - E\right) \qquad (1.2)$$

A quantum well is a 2D system in which the electron is free to move in the x-y direction but quantized in the z direction. As seen in Table 1.1, this results in a sequence of 2D energy subbands and a step-like dependence of the DOS.

In contrast to quantum wells, electrons in 1D systems are limited in two directions and only allowed to travel freely in one direction. Thus, the 1D system's sub band was identical to those described in the 2D system, with a sequence of spikes as seen in Table 1.1. The DOS for 1D system is stated by equation (1.3):

$$D(E) = \frac{m^*}{\pi\hbar}\sqrt{\frac{m^*}{2(E_g - E)}} \qquad (1.3)$$

Quantum dots (QDs) are classified as a 0D system, meaning that carriers are confined in three different directions. At all states, the energies are discrete, as seen in Table 1.1. QDs have zero dimensional and the charge carriers confined in three dimensions be a prominently factor why it is being chosen in this study besides their unique properties in electrical and optical. Furthermore, QDs has expanded its usage on a lot of things in this world. For example, QDs LED which is used to produce inexpensive, industrial quality white light. It has made an improvement over traditional LED which is phosphor integration with quantum dot's ability to absorb and emit at any desired wavelength. The QDs LED will produce white light by intermixing red, green, and blue emitting dots homogeneously within the phosphor, difficult to accomplish with the traditional LED-phosphor set up. Figure 1.1 shows the example of QDs solution with different colour of emission.

Table 1.1: Nanomaterials are classified as 3D, 2D, 1D and 0D which according to their density of state and quantum confinement.

Type of nanomaterial	Density of State (DOS)	Quantum confinement
3 dimensional (3D)	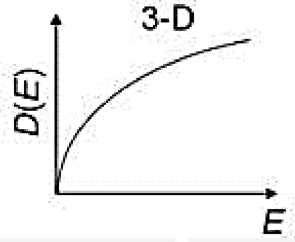	The charge carriers are not confined in any dimension.
2 dimensional (2D)	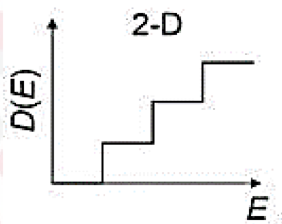	The charge carriers confined in one dimension.
1 dimensional (1D)	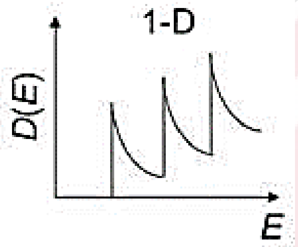	The charge carriers confined in two dimensions.
0 dimensional (0D)	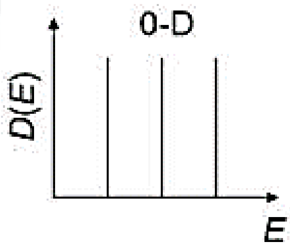	The charge carriers confined in all three dimensions.

Source: Roduner *et al*., 2006

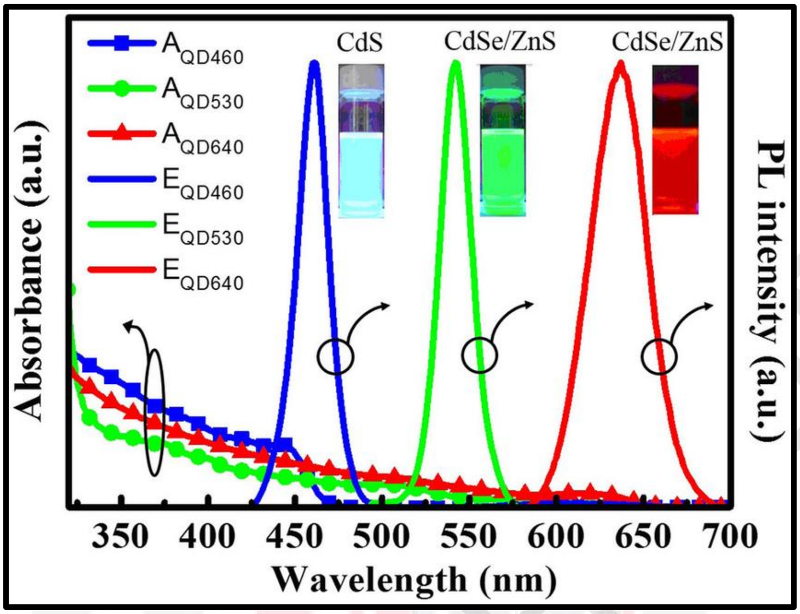

Figure 1.1: QDs emit at colour in the region of visible wavelength. (Han *et al.,* 2014)

Other than that, the QDs solar cell is the one of the QDs applications. Nowadays, solar cells are made of semiconductors and the materials to produce it are costly. The QDs solar cell is the solar cell pattern that uses QDs as the photovoltaic layer. QDs have a tunable bandgap beyond a wide energy level by adjustment of the QDs size. This benefit of QDs makes it interesting in making the multi junction solar cell.

In recent years, many reported workers had prepared QDs with different semiconductors such as zinc tellurite (ZnTe) (Cheng *et al*., 2015), cadmium selenide (CdSe) (Selvan *et al*., 2005) and indium arsenide (InAs) (Tossoun *et al*., 2019). (Yuwen *et al*., 2013) had claimed that the different emission of QDs can be synthesized if choosing the suitable composition and tuning the size of QDs. The difference of emission in near-infrared (NIR) with tunable size is one the reason why PbS QDs from the IV-VI semiconductor nanocrystal had been selected in this research (Wang *et al*., 2012).

Meanwhile the technology and applications of QDs grow faster in the past few years, the demand to produce more sufficient QDs to achieve the application requirement is important to the research field all around the world. So, to produce the sufficient QDs, many researchers had altered the QDs properties by capping the QDs with organic/inorganic material to form core/shell QDs for improving the QDs properties to encounter the need of applications. Figure 1.2 shows the illustration of core/shell QDs.

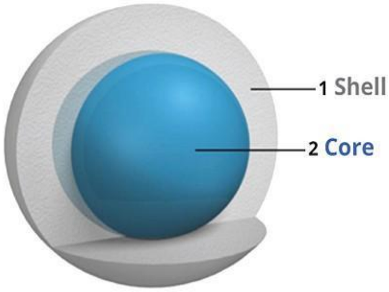

Figure 1.2: The figure shows the cross-sectional image of core/shell QDs. (Neo *et al.,* 2010)

Many recent works had made an effort to synthesis core/shell quantum dots with different types of core shell such as type-I core/shell QDs CdSe/ZnS (Zhu *et al*., 2010), type-II core/shell QDs CdTe/CdSe (Kim *et al*., 2003) and reverse type-I core/shell QDs InAs/GaAs (Hospodková *et al*., 2011). The optical properties of core QDs can be improved by passivating the core with the shell material that has a larger band gap than core which is these properties fits to type-I core/shell QDs (Reiss *et al*., 2009).

Manganese (Mn) chalcogenides like manganese telluride (MnTe) were chosen as the material to encapsulate the PbS core QDs in this experiment. Mn-chalcogenides take an interest in this topic due to their exciting electronic and magneto-optoelectronic properties besides their usefulness in less toxicity of the metal cores (Aplesnin *et al*., 2007). Moreover, MnTe also play an important role in this research due to their interesting characteristics in quantum confinement and size-dependent photoemission (Li *et al*., 2020).

In this thesis, we had reported how to synthesize and PbS QDs capped with MnTe shell and characterize their structural and optical properties.

1.2 Problem Statement

In past decades, numerous researchers have focused to improve efficiency and produce optical properties of devices by the synthesized QDs capped with organic ligands. Nevertheless, the fluorescence quantum yields of QDs that capped with organic ligands was low due to the surface defects and surface trap state (Samuel *et al*., 2018). This challenge can be handled by producing core shell QDs by building a semiconductor shell layer around the core of QDs. The shell will protect the core's surface from oxidation while also providing stability to improve the luminescence qualities. This is because smoothing of core-surface defects causes defect saturation and dangling bonds, which can lead to non-radiative electron-hole pair recombination.

Core/shell QDs have been synthesised using a variety of techniques, including organometallic and electrochemical approaches (Reilly *et al*., 2014; Gopalakrishnan *et al*., 2015). On the other hand, these approaches required long and complex synthetic procedures as well as create low-quality structures. Organometallic method is often utilized to fabricate core/shell QDs, which requires a high temperature and a long procedure. However, high-temperature synthesis which is controlled by solvent boiling points, results in a produce high defect density.

Electrochemical synthesis has been extensively employed to synthesis core/shell QDs because of their benefits which include the use of an aqueous solvent, deposition at ambient temperature, and low cost. Regrettably, using an electrochemical approach to generate core/shell QDs was problematic due to the complexity of generating electrically addressable nanoparticle arrays. This inspires us to use a different strategy to make core shell QDs: an aqueous synthesis process that is both easy and successful.

This aqueous synthesis approach uses low cost of production because this method utilised water as a solvent. This technique also applicable for lead chalcogenide. PbS core QDs were synthesised as a control sample in this example. By introducing MnTe precursor and form MnTe shell. As a result, significant attention has been focused to synthesizing core/shell QDs by layering a MnTe shell over a PbS core in order to analyze the effect of the MnTe shell on structural and optical properties.

PbS was chosen in this research because of its large exciton Bohr radius. PbS has an exciton Bohr radius of 18 nm (Fu *et al*., 2011), which is relatively big compared to other semiconductors as CdS and CdTe QDs, which have Bohr radius of 5.8 nm and 7.3 nm (Arellano *et al*., 2013; Khatei *et al*., 2012). However, the quality of luminescence of core PbS QDs was very low due to oxidation on the surface of the core.

MnTe was chosen as the capping material to prevent oxidation on the surface of the PbS core due to its unique properties in structural and optical. Beside that, the wide band gap MnTe shell that capped PbS core QDs will yield type-I core/shell QDs. In past decades, type-I core/shell QDs which is has wide band gap shell like PbS/CdS (Lai *et al*., 2014) and PbS/MnS (Zaini *et al*., 2020) had been produced by other researchers. These wide band gap shells improve the light harvesting properties of visible light when used as Quantum Dots Solar Cell (QDSC) (Aissat *et al*., 2017)

In order to verify the growth of the MnTe shell on PbS core in core/shell samples, HRTEM and EDX analysis can be performed to characterize the size of particles and the elemental composition. In order to understand the effects of temperature on PbS QDs and PbS/MnTe core shell QDs, the temperature dependence of PL emission of PbS QDs and PbS/MnTe core shell QDs was investigated. Although all electrical devices are designed to work ideally at ambient temperature, their capacity to work well at any temperature is still developing. The dominant carrier recombination in PbS QDs and PbS/MnTe core core QDs can be investigated by varying the temperature in PL emission. Furthermore, the information about low energy state of the QDs can be studied by conducting PL measurements at low temperature (Valerini *et al*., 2005)

1.3 Research Objectives

The goals of this research are as follows:

i. to synthesize PbS QDs capping with MnTe with different shell thickness by using aqueous method.
ii. to study the morphology and PL properties of PbS/MnTe core/shell QDs.
iii. to assess the effect of electron-phonon interaction towards bandgap modulation via PL temperature dependence

REFERENCES

Adim, N., Caid, M., Rached, D., & Cheref, O. (2020). Computational study of structural, electronic, magnetic and optical properties of (ZnTe)m/(MnTe)n superlattices. *Journal of Magnetism and Magnetic Materials*, 499, 166314.

Allen, J., Lucovsky, G., & Mikkelsen, J. (1977). Optical properties and electronic structure of crossroads material MnTe. *Solid State Communications*, 24(5), 367-370.

Ali Farhan Ogaili, A., S. Al-Ameen, E., Salman Kadhim, M., & Nazar Mustafa, M. (2020). Evaluation of mechanical and electrical properties of GFRP composite strengthened with hybrid nanomaterial fillers. *AIMS Materials Science*, *7*(1), 93-102.

Aminorroaya Yamini, S., Wang, H., Gibbs, Z., Pei, Y., Mitchell, D., Dou, S., & Snyder, G. (2014). Thermoelectric performance of tellurium-reduced quaternary p-type lead–chalcogenide composites. *Acta Materialia*, *80*, 365-372.

Aplesnin, S., Ryabinkina, L., Romanova, O., Balaev, D., Demidenko, O., Yanushkevich, K., & Miroshnichenko, N. (2007). Effect of the orbital ordering on the transport and magnetic properties of MnSe and MnTe. *Physics of The Solid State*, *49*(11), 2080-2085.

Arellano, I., Mangadlao, J., Ramiro, I., & Suazo, K. (2010). 3-component low temperature solvothermal synthesis of colloidal cadmium sulfide quantum dots. *Materials Letters*, *64*(6), 785-788.

Ashraf, M., Salah, N., Rafat, M., & Khana, Z. (2017). Synthesis and characterization of Indium doped Lead chalcogenides(PbSe)100−xInx thin films composed of QDs. *Journal Of Alloys And Compounds*, *701*, 850-857.

Aubert, T., Cirillo, M., Flamee, S., Van Deun, R., Lange, H., Thomsen, C., & Hens, Z. (2013). Homogeneously Alloyed CdSe1–xSx Quantum Dots (0 ≤ x ≤ 1): An Efficient Synthesis for Full Optical Tunability. *Chemistry of Materials*, *25*(12), 2388-2390.

Bae, W., Padilha, L., Park, Y., McDaniel, H., Robel, I., Pietryga, J., & Klimov, V. (2013). Controlled Alloying of the Core–Shell Interface in CdSe/CdS Quantum Dots for Suppression of Auger Recombination. ACS Nano, 7(4), 3411-3419.

Bakueva, L., Gorelikov, I., Musikhin, S., Zhao, X., Sargent, E., & Kumacheva, E. (2004). PbS Quantum Dots with Stable Efficient Luminescence in the Near-IR Spectral Range. *Advanced Materials*, *16*(11), 926-929.

Benayas, A., Ren, F., Carrasco, E., Marzal, V., del Rosal, B., & Gonfa, B. *et al*. (2015). PbS/CdS/ZnS Quantum Dots: A Multifunctional Platform for In Vivo Near-Infrared Low-Dose Fluorescence Imaging. Advanced Functional Materials, 25(42), 6650-6659.

Bi, J., Lu, H., Sreenivasan, M., & Teo, K. (2009). Exchange bias in zinc-blende CrTe–MnTe bilayer. *Applied Physics Letters*, *94*(25), 252504.

Brokmann, X., Coolen, L., Dahan, M., & Hermier, J. (2004). Measurement of the Radiative and Nonradiative Decay Rates of Single CdSe Nanocrystals through a Controlled Modification of their Spontaneous Emission. *Physical Review Letters*, *93*(10).

Brus, L. (1983). A simple model for the ionization potential, electron affinity, and aqueous redox potentials of small semiconductor crystallites. *The Journal of Chemical Physics*, *79*(11), 5566-5571.

Brus, L. (1984). Electron–electron and electron-hole interactions in small semiconductor crystallites: The size dependence of the lowest excited electronic state. *The Journal of Chemical Physics*, *80*(9), 4403-4409.

Brus, L. (1986). Electronic wave functions in semiconductor clusters: experiment and theory. *The Journal of Physical Chemistry*, *90*(12), 2555-2560

Cassidy, J., & Zamkov, M. (2020). Nanoshell quantum dots: Quantum confinement beyond the exciton Bohr radius. *The Journal of Chemical Physics*, *152*(11), 110902.

Che, D., Zhu, X., Wang, H., Duan, Y., Zhang, Q., & Li, Y. (2016). Aqueous synthesis of high bright and tunable near-infrared AgInSe 2 –ZnSe quantum dots for bioimaging. *Journal of Colloid and Interface Science*, *463*, 1-7.

Chen, G., Seo, J., Yang, C., & Prasad, P. (2013). Nanochemistry and nanomaterials for photovoltaics. *Chemical Society Reviews*, 42(21), 8304.

Chen, Y., & Rosenzweig, Z. (2002). Luminescent CdS Quantum Dots as Selective Ion Probes. *Analytical Chemistry*, *74*(19), 5132-5138.

Cheng, T., Li, D., Li, J., Ren, B., Wang, G., & Cheng, J. (2015). Aqueous synthesis of high-fluorescence ZnTe quantum dots. *Journal of Materials Science: Materials In Electronics*, *26*(6), 4062-4068.

Chiodini, N., Paleari, A., DiMartino, D., & Spinolo, G. (2002). SnO2 nanocrystals in SiO2: A wide-band-gap quantum-dot system. *Applied Physics Letters*, *81*(9), 1702-1704.

Chung, H., Choi, H., Kim, D., Jeong, S., & Kim, J. (2015). Size Dependence of Excitation-Energy-Related Surface Trapping Dynamics in PbS Quantum Dots. *The Journal of Physical Chemistry C*, *119*(13), 7517-7524.

Cristea, M., & Niculescu, E. (2012). Hydrogenic impurity states in CdSe/ZnS and ZnS/CdSe core-shell nanodots with dielectric mismatch. *The European Physical Journal B*, *85*(6).

Cui, W., Qi, Y., Liu, L., Rana, D., Hu, J., & Liang, Y. (2012). Synthesis of PbS–K2La2Ti3O10 composite and its photocatalytic activity for hydrogen production. *Progress in Natural Science: Materials International*, *22*(2), 120-125.

Dancus, I., Vlad, V. I., Petris, A., Gaponik, N., Lesnyak, V., & Eychmüller, A. (2010). Optical limiting and phase modulation in CdTe nanocrystal devices. *Journal of Optoelectronics and Advanced Materials*, *12*(1), 119.

Dey, P., Paul, J., Bylsma, J., Karaiskaj, D., Luther, J., Beard, M., & Romero, A. (2013). Origin of the temperature dependence of the band gap of PbS and PbSe quantum dots. *Solid State Communications*, *165*, 49-54.

Du, H., Chen, C., Krishnan, R., Krauss, T., Harbold, J., & Wise, F. *et al*. (2002). Optical Properties of Colloidal PbSe Nanocrystals. *Nano Letters*, *2*(11), 1321-1324.

Efros, A. L., & Efros, A. L. (1982). Interband absorption of light in a semiconductor sphere. *Soviet Physics Semiconductors-Ussr, 16*(7), 772-775.

Ekimov, A. I., & Onushchenko, A. A. (1981). Quantum size effect in 3-dimensional microscopic semiconductor crystals. *JETP Lett., 34*, 345-349.

El-Ballouli, A., Alarousu, E., Bernardi, M., Aly, S., Lagrow, A., Bakr, O., & Mohammed, O. (2014). Quantum Confinement-Tunable Ultrafast Charge Transfer at the PbS Quantum Dot and Phenyl-C61-butyric Acid Methyl Ester Interface. *Journal of The American Chemical Society*, 136(19), 6952-6959.

Fu, X., Pan, Y., Wang, X., & Lombardi, J. (2011). Quantum confinement effects on charge-transfer between PbS quantum dots and 4-mercaptopyridine. *The Journal of Chemical Physics*, *134*(2), 024707.

Gaponenko, M., Lutich, A., Tolstik, N., Onushchenko, A., Malyarevich, A., Petrov, E., & Yumashev, K. (2010). Temperature-dependent photoluminescence of PbS quantum dots in glass: Evidence of exciton state splitting and carrier trapping. *Physical Review B*, *82*(12).

Gélinas, G., Lanacer, A., Leonelli, R., Masut, R., & Poole, P. (2010). Carrier thermal escape in families of InAs/InP self-assembled quantum dots. *Physical Review B*, *81*(23).

Gopalakrishnan, D., Damien, D., Li, B., Gullappalli, H., Pillai, V., Ajayan, P., & Shaijumon, M. (2015). Electrochemical synthesis of luminescent MoS2 quantum dots. *Chemical Communications*, *51*(29), 6293-6296.

Haldar, S., Dixit, V., Vashisht, G., Porwal, S., & Sharma, T. (2017). The effect of magnetic field on free and bound exciton luminescence in GaAs/AlGaAs multiple quantum well structures: a quantitative study on the estimation of ultra-low disorder. *Journal of Physics D: Applied Physics*, *50*(33), 335107.

Han, H., Lin, C., Tsai, Y., Chen, H., Chen, K., & Yeh, Y. *et al*. (2014). A Highly Efficient Hybrid GaAs Solar Cell Based on Colloidal-Quantum-Dot-Sensitization. *Scientific Reports*, *4*(1).

Hartmann, J., Kany, F., Chautain, F., Rouvière, J., Wasiela, A., & Mariette, H. (1998). Structural and optical properties of CdTe/MnTe tilted superlattices grown on vicinal surfaces. *Journal of Crystal Growth*, 184-185, 279-282.

Hospodková, A., Pangrác, J., Oswald, J., Hazdra, P., Kuldová, K., Vyskočil, J., & Hulicius, E. (2011). Influence of strain reducing layers on electroluminescence and photoluminescence of InAs/GaAs QD structures. *Journal of Crystal Growth*, *315*(1), 110-113.

Hsu, W., Lin, K., & Hsieh, W. (2007). Reducing exciton-longitudinal-optical phonon interaction with shrinking ZnO quantum dots. *Applied Physics Letters*, *91*(18), 181913.

Hu, H., Wang, K., Long, H., Liu, W., Wang, B., & Lu, P. (2015). Precise Determination of the Crystallographic Orientations in Single ZnS Nanowires by Second-Harmonic Generation Microscopy. *Nano Letters*, *15*(5), 3351-3357.

Imai, Y., Mukaida, M., & Tsunoda, T. (2001). Calculation of electronic energy and density of state of iron-disilicides using a total-energy pseudopotential method, CASTEP. *Thin Solid Films*, *381*(2), 176-182.

Jiao, Y., Gao, X., Lu, J., Chen, Y., Zhou, J., & Li, X. (2012). A novel method for PbS quantum dot synthesis. *Materials Letters*, *72*, 116-118.

Karan, S., Majumder, M., & Mallik, B. (2012). Controlled surface trap state photoluminescence from CdS QDs impregnated in poly (methyl methacrylate). Photochemical & Photobiological Sciences, 11(7), 1220.

Karim, M., Balaban, M., & Ünlü, H. (2019). Strain Effects on the Band Gap and Diameter of CdSe Core and CdSe/ZnS Core/Shell Quantum Dots at Any Temperature. *Advances in Materials Science and Engineering*, *2019*, 1-10.

Khatei, J., Suchand Sandeep, C., Philip, R., & Koteswara Rao, K. (2012). Near-resonant two-photon absorption in luminescent CdTe quantum dots. *Applied Physics Letters*, *100*(8), 081901.

Kim, D., Kim, D., Lee, J., & Grossman, J. (2013). Impact of Stoichiometry on the Electronic Structure of PbS Quantum Dots. *Physical Review Letters*, *110*(19).

Kim, E., Kim, J., Kim, H., Lee, B., Choi, E., & In, S. (2015). Carcinogenic activity of PbS quantum dots screened using exosomal biomarkers secreted from HEK293 cells. *International Journal of Nanomedicine*, 5513.

Kim, S., Fisher, B., Eisler, H., & Bawendi, M. (2003). Type-II Quantum Dots: CdTe/CdSe(Core/Shell) and CdSe/ZnTe(Core/Shell) Heterostructures. *Journal of The American Chemical Society*, *125*(38), 11466-11467.

Kirchartz, T., Taretto, K., & Rau, U. (2009). Efficiency Limits of Organic Bulk Heterojunction Solar Cells. *The Journal of Physical Chemistry C*, *113*(41), 17958-17966.

Koo, B. H., Chon, G. B., Lim, H. S., Lee, C. G., & Yao, T. (2006). Effect of lattice mismatch on the properties of self-assembled InAs/InAlAs/InP quantum dots. *Journal of the Korean Physical Society*, *49*(3), 873-876.

Kriegner, D., Výborný, K., Olejník, K., Reichlová, H., Novák, V., & Marti, X. *et al*. (2016). Multiple-stable anisotropic magnetoresistance memory in antiferromagnetic MnTe. *Nature Communications*, *7*(1).

Kulakovich, O., Strekal, N., Yaroshevich, A., Maskevich, S., Gaponenko, S., & Nabiev, I. *et al*. (2002). Enhanced Luminescence of CdSe Quantum Dots on Gold Colloids. *Nano Letters*, *2*(12), 1449-1452.

Kyhm, K., Kim, J., Kim, S., & Yang, H. (2007). Gain dynamics and excitonic transition in CdSe colloidal quantum dots. *Optical Materials*, *30*(1), 158-160.

Lai, L., Protesescu, L., Kovalenko, M., & Loi, M. (2014). Sensitized solar cells with colloidal PbS–CdS core–shell quantum dots. *Phys. Chem. Chem. Phys.*, *16*(2), 736-742.

Lei, D., Shen, Y., Feng, Y., & Feng, W. (2012). Recent progress in the fields of tuning the band gap of quantum dots. *Science China Technological Sciences*, *55*(4), 903-912.

Li, L., Li, H., Li, J., Wu, H., Yang, L., Zhang, W., & Chang, H. (2020). Chemical Vapor Deposition-Grown Nonlayered α-MnTe Nanosheet for Photodetectors with Ultrahigh Responsivity and External Quantum Efficiency. *Chemistry of Materials*, *33*(1), 338-346.

Li, Z., Dong, J., Sun, F., Hirono, S., & Li, J. (2017). Significant Enhancement of the Thermoelectric Performance of Higher Manganese Silicide by Incorporating MnTe Nanophase Derived from Te Nanowire. *Chemistry of Materials*, *29*(17), 7378-7389.

Lin, Z., Lai, Y., Hu, R., Li, J., Du, R., & Lin, C. (2010). A highly efficient ZnS/CdS@TiO2 photoelectrode for photogenerated cathodic protection of metals. *Electrochimica Acta*, *55*(28), 8717-8723.

Litvin, A., Parfenov, P., Ushakova, E., Simões Gamboa, A., Fedorov, A., & Baranov, A. (2014). Size and Temperature Dependencies of the Low-Energy Electronic Structure of PbS Quantum Dots. *The Journal of Physical Chemistry C*, *118*(35), 20721-20726.

Martynenko, I., Baimuratov, A., Osipova, V., Kuznetsova, V., Purcell-Milton, F., & Rukhlenko, I. *et al*. (2018). Excitation Energy Dependence of the Photoluminescence Quantum Yield of Core/Shell CdSe/CdS Quantum Dots and Correlation with Circular Dichroism. *Chemistry of Materials*, *30*(2), 465-471.

Molaei, M., Abbasi, S., Karimipour, M., & Dehghan, F. (2018). A simple UV-assisted, room temperature approach for synthesis of water soluble PbS and PbS/CdS core-shell QDs. *Materials Chemistry and Physics*, *216*, 186-190.

Mondal, S., Bera, S., Narender, G., & Ray, S. (2012). CdSe quantum dots-poly(3-hexylthiophene) nanocomposite sensors for selective chloroform vapor detection at room temperature. *Applied Physics Letters*, *101*(17), 173108.

Neo, M., Venkatram, N., Li, G., Chin, W., & Ji, W. (2010). Synthesis of PbS/CdS Core−Shell QDs and their Nonlinear Optical Properties. *The Journal of Physical Chemistry C*, *114*(42), 18037-18044.

Pan, Y., Li, Y., Zhao, Y., & Akins, D. (2015). Synthesis and Characterization of Quantum Dots: A Case Study Using PbS. *Journal of Chemical Education*, *92*(11), 1860-1865.

Pan, Z., Zhang, H., Cheng, K., Hou, Y., Hua, J., & Zhong, X. (2012). Highly Efficient Inverted Type-I CdS/CdSe Core/Shell Structure QD-Sensitized Solar Cells. *ACS Nano*, *6*(5), 3982-3991.

Patel, J., Jain, B., Singh, A., Susan, M., & Jean-Paul, L. (2020). Mn-Doped ZnS Quantum dots–An Effective Nanoscale Sensor. *Microchemical Journal*, *155*, 104755.

Pourahmad, A. (2014). Preparation and spectroscopic studies of PbS/nanoMCM-41 nanocomposite. *Arabian Journal of Chemistry*, *7*(5), 788-792.

Qiao, Z., Zhang, Y., Zhou, L., & Xire, Q. (2007). Shape Control of PbS Crystals under Microwave Irradiation. *Crystal Growth & Design*, *7*(12), 2394-2396.

Rahimi, F., Anbia, M., & Farahi, M. (2021). Aqueous synthesis of L- methionine capped PbS quantum dots for sensitive detection and quantification of arsenic (III). *Journal of Photochemistry and Photobiology A: Chemistry*, *417*, 113361.

Reed, M., Randall, J., Aggarwal, R., Matyi, R., Moore, T., & Wetsel, A. (1988). Observation of discrete electronic states in a zero-dimensional semiconductor nanostructure. *Physical Review Letters*, *60*(6), 535-537.

Reilly, N., Wehrung, M., O'Dell, R., & Sun, L. (2014). Ultrasmall colloidal PbS quantum dots. *Materials Chemistry and Physics*, *147*(1-2), 1-4.

Reilly, N., Wehrung, M., O'Dell, R., & Sun, L. (2014). Ultrasmall colloidal PbS quantum dots. *Materials Chemistry and Physics*, *147*(1-2), 1-4.

Reiss, P., Protière, M., & Li, L. (2009). Core/Shell Semiconductor Nanocrystals. *Small*, *5*(2), 154-168.

Ren, Y., Yang, J., Jiang, Q., Zhang, D., Zhou, Z., & Li, X. *et al*. (2017). Synergistic effect by Na doping and S substitution for high thermoelectric performance of p-type MnTe. *Journal of Materials Chemistry C*, *5*(21), 5076-5082.

Roduner, E. (2006). Size matters: why nanomaterials are different. Chemical Society Reviews, 35(7), 583.

Rosen, S., Schwartz, O., & Oron, D. (2010). Transient Fluorescence of the Off State in Blinking CdSe/CdS/ZnS Semiconductor Nanocrystals Is Not Governed by Auger Recombination. *Physical Review Letters*, *104*(15).

Samuel, B., Mathew, S., Anand, V., Correya, A., Nampoori, V., & Mujeeb, A. (2018). Surface defect assisted broad spectra emission from CdSe quantum dots for white LED application. *Materials Research Express*, *5*(2), 025009.

Sanguinetti, S., Poliani, E., Bonfanti, M., Guzzi, M., Grilli, E., Gurioli, M., & Koguchi, N. (2006). Electron-phonon interaction in individual strain-free GaAs⁄Al0.3Ga0.7As quantum dots. *Physical Review B*, *73*(12).

Selopal, G., Zhao, H., Wang, Z., & Rosei, F. (2020). Core/Shell Quantum Dots Solar Cells. Advanced Functional Materials, 30(13), 1908762.

Selvan, S., Tan, T., & Ying, J. (2005). Robust, Non-Cytotoxic, Silica-Coated CdSe Quantum Dots with Efficient Photoluminescence. *Advanced Materials*, *17*(13), 1620-1625.

Su, G., Liu, C., Deng, Z., Zhao, X., & Zhou, X. (2017). Size-dependent photoluminescence of PbS QDs embedded in silicate glasses. *Optical Materials Express*, *7*(7), 2194.

Tang, Y., Li, Z., Li, Z. T., Li, J. S., Yu, S. D., & Rao, L. S. (2017). Enhancement of luminous efficiency and uniformity of CCT for quantum dot-converted LEDs by incorporating with ZnO nanoparticles. *IEEE Transactions on Electron Devices*, *65*(1), 158-164.

Tisdale, W., & Zhu, X. (2010). Artificial atoms on semiconductor surfaces. *Proceedings of The National Academy of Sciences*, *108*(3), 965-970.

Tossoun, B., Kurczveil, G., Zhang, C., Descos, A., Huang, Z., & Beling, A. *et al*. (2019). Indium arsenide quantum dot waveguide photodiodes heterogeneously integrated on silicon. *Optica*, *6*(10), 1277.

Tubtimtae, A., Arthayakul, K., Teekwang, B., Hongsith, K., & Choopun, S. (2013). MnTe semiconductor-sensitized boron-doped TiO2 and ZnO photoelectrodes for solar cell applications. *Journal of Colloid and Interface Science*, *405*, 78-84.

Turyanska, L., Moro, F., Knott, A., Fay, M., Bradshaw, T., & Patanè, A. (2013). Paramagnetic, Near-Infrared Fluorescent Mn-Doped PbS Colloidal

Nanocrystals. *Particle & Particle Systems Characterization*, *30*(11), 945-949.

Turyanska, L., Patanè, A., Henini, M., Hennequin, B., & Thomas, N. (2007). Temperature dependence of the photoluminescence emission from thiol-capped PbS quantum dots. *Applied Physics Letters*, *90*(10), 101913.

Valerini, D., Cretí, A., Lomascolo, M., Manna, L., Cingolani, R., & Anni, M. (2005). Temperature dependence of the photoluminescence properties of colloidalCdSe⁄ZnScore/shell quantum dots embedded in a polystyrene matrix. *Physical Review B*, *71*(23).

Valerini, D., Cretí, A., Lomascolo, M., Manna, L., Cingolani, R., & Anni, M. (2005). Temperature dependence of the photoluminescence properties of colloidalCdSe⁄ZnScore/shell quantum dots embedded in a polystyrene matrix. *Physical Review B*, *71*(23).

Vasilevskiy, M., Anda, E., & Makler, S. (2004). Electron-phonon interaction effects in semiconductor quantum dots: A nonperturabative approach. *Physical Review B*, *70*(3).

Vorrath, T., & Blmel, R. (2003). Electronic structure of three-dimensional quantum dots. *The European Physical Journal B - Condensed Matter*, *32*(2), 227-235.

Wang, D., Qian, J., Cai, F., He, S., Han, S., & Mu, Y. (2012). 'Green'-synthesized near-infrared PbS quantum dots with silica–PEG dual-layer coating: ultrastable and biocompatible optical probes forin vivoanimal imaging. *Nanotechnology*, *23*(24), 245701.

Wang, D., Qian, J., Cai, F., He, S., Han, S., & Mu, Y. (2012). 'Green'-synthesized near-infrared PbS quantum dots with silica–PEG dual-layer coating: ultrastable and biocompatible optical probes forin vivoanimal imaging. *Nanotechnology*, *23*(24), 245701.

Wang, Z., Ren, X., Wang, L., Cui, G., Wang, H., & Sun, X. (2018). A hierarchical CoTe2–MnTe2 hybrid nanowire array enables high activity for oxygen evolution reactions. *Chemical Communications*, *54*(78), 10993-10996.

Wei, G., Yan, Z., Tian, J., Zhao, G., Guang, S., & Xu, H. (2020). Efficient Polymer Pendant Approach toward High Stable Organic Fluorophore for Sensing Ultratrace Hg2+ with Improved Biological Compatibility and Cell Permeability. *Analytical Chemistry*, *92*(4), 3293-3301.

Wichiansee, W., Nordin, M., Green, M., & Curry, R. (2011). Synthesis and optical characterization of infra-red emitting mercury sulfide (HgS) quantum dots. *Journal of Materials Chemistry*, *21*(20), 7331.

Wu, W., Chakrabortty, S., Guchhait, A., Wong, G., Dalapati, G., Lin, M., & Chan, Y. (2016). Solution-Processed 2D PbS Nanoplates with Residual Cu2S Exhibiting Low Resistivity and High Infrared Responsivity. *Chemistry of Materials*, *28*(24), 9132-9138.

Yang, S. S., Ren, C. L., Zhang, Z. Y., Hao, J. J., Hu, Q., & Chen, X. G. (2011). Aqueous synthesis of CdTe/CdSe core/shell quantum dots as pH-sensitive fluorescence probe for the determination of ascorbic acid. *Journal of fluorescence*, *21*(3), 1123-1129.

Yang, X., Yang, J., Khan, J., Deng, H., Yuan, S., & Zhang, J. *et al*. (2020). Hydroiodic Acid Additive Enhanced the Performance and Stability of PbS-QDs Solar Cells via Suppressing Hydroxyl Ligand. Nano-Micro Letters, 12(1).

Yu, Y., Zhang, K., & Sun, S. (2013). Effect of ligands on the photoluminescence properties of water-soluble PbS quantum dots. *Journal of Molecular Structure*, *1031*, 194-200.

Yuwen, L., & Wang, L. (2013). Nanoparticles and quantum dots. *Handbook of Chalcogen Chemistry: New Perspectives in Sulfur, Selenium and Tellurium*, *2*, 232-269.

Zeng, Y., Ye, Z., Liu, F., Li, D., Lu, Y., & Jaeger, W. *et al*. (2008). Controllable Growth and Characterization of ZnO/MgO Quasi Core−Shell Quantum Dots. *Crystal Growth & Design*, *9*(1), 263-266.

Zhang, L., Chen, L., Liu, J., Fang, X., & Zhang, Z. (2016). Effect of morphology of carbon nanomaterials on thermo-physical characteristics, optical properties and photo-thermal conversion performance of nanofluids. *Renewable Energy*, *99*, 888-897.

Zhao, X., Gorelikov, I., Musikhin, S., Cauchi, S., Sukhovatkin, V., Sargent, E., & Kumacheva, E. (2005). Synthesis and Optical Properties of Thiol-Stabilized PbS Nanocrystals. *Langmuir*, *21*(3), 1086-1090.

Zhao, Z., Yi, C., Lantz, K., & Stiff-Roberts, A. (2007). Effect of donor-complex-defect-induced dipole field on InAs⁄GaAs quantum dot infrared photodetector activation energy. *Applied Physics Letters*, *90*(23), 233511.

Zhu, H., Song, N., & Lian, T. (2010). Controlling Charge Separation and Recombination Rates in CdSe/ZnS Type I Core−Shell Quantum Dots by

Shell Thicknesses. *Journal of The American Chemical Society*, *132*(42), 15038-15045.

Zhuang, T., Fan, F., Gong, M., & Yu, S. (2012). Cu1.94S nanocrystal seed mediated solution-phase growth of unique Cu2S–PbS heteronanostructures. *Chemical Communications*, *48*(78), 9762.

Halim, N. D., Zaini, M. S., Talib, Z. A., Liew, J. Y. C., & Kamarudin, M. A. (2022). Study of the Electron-Phonon Coupling in PbS/MnTe Quantum Dots Based on Temperature-Dependent Photoluminescence. *Micromachines*, *13*(3), 443